



ELSEVIER



CrossMark

Procedia Manufacturing

Volume 1, 2015, Pages 619–627

43rd Proceedings of the North American Manufacturing Research  
Institution of SME <http://www.sme.org/namrc>



# High-Precision Finishing Hard Steel Surfaces Using Cutting, Abrasive and Burnishing Operations

Wit Grzesik<sup>1\*</sup>, Jöel Rech<sup>2</sup> and Krzysztof Żak<sup>1</sup>

<sup>1</sup> *Department of Manufacturing Engineering and Production Automation  
Opole University of Technology, Opole, Poland*

<sup>2</sup> *Tribology and System Dynamics Laboratory's (LTDS)*

*École Nationale d'Ingénieurs de Saint-Etienne*

*Université de Lyon, Saint-Etienne, France*

*w.grzesik@po.opole.pl, joel.rech@enise.fr, k.zak@po.opole.pl*

## Abstract

This paper presents the technological and functional capabilities of surface textures produced by high-precision cutting, abrasive and ball burnishing operations on hardened steel parts of about 60 HRC hardness. Special focus was placed on surface textures generated by hard turning, belt grinding and ball burnishing operations which are characterized by the Sz roughness parameter of about 1.3  $\mu\text{m}$  and distinctly different values of the Sa parameter. Apart from the standard 2D and 3D roughness parameters, the fractal and motif parameters were analyzed.

*Keywords:* Hardened steel, hard turning, belt grinding, ball burnishing, surface roughness, surface texture

## 1 Introduction

Strong technological demands on the quality, functionality and reliability of machined parts have influenced the visible progress in surface metrology. As a result, the functional surfaces produced by modern manufacturing processes (including hard part machining) can be characterized with a higher accuracy using a number of the field parameters (S-parameters and V-parameters sets) (Jiang and Whitehouse, 2012). A marked achievement in this area has been seen in the standardization of 3D roughness parameters (Jiang and Whitehouse, 2012; De Chiffre et. al., 2000; Lonardo et. al., 1996). Among innovative machining technologies, precision machining with  $R_z = 2.5\text{--}4\ \mu\text{m}$  and high-precision machining with  $R_z < 1\ \mu\text{m}$  of hardened steels (45-60 HRC) with CBN cutting tool materials seems to be the leading one. They have been developed with a special consideration to automotive, hydraulic and die and mold industry sectors (Tönshoff et. al., 2000; Klocke, 2011) due to high

\* Corresponding author. Tel.: +48-774498459; fax: +48-774499927. E-mail address: w.grzesik@po.opole.pl.

flexibility, possible complete machining, lesser ecological impact and higher MRR (König et al., 1993; Davim 2011). Initially, hard machining was introduced as a replacement of more energy consuming and environmentally hazardous grinding (Klocke et al., 2005). In this aspect, the functionality of the machined surfaces produced by cutting and grinding operations should be taken into account. This is because hard turning and grinding, as well as other abrasive finishing operations, generate different surface structures which influence distinctly their functional properties. Previously, investigations were based on 2D height and amplitude parameters and the relevant BACs shapes (Klocke et al., 2005). However, a dissimilarity between the hard turned and ground surface topographies was revealed although the values of the Ra or Rz parameters are comparable. The 2D and 3D comparison of precision hard turning and belt grinding with a contribution to bearing area parameters was established by Grzesik et al. (Grzesik et al., 2007). Further, it was extended to superfinishing and ball burnishing operations (Grzesik and Žak, 2012) in order to investigate their influence on the modification of the texture of a CBN turned surface. It is evident that future investigations of surface finish and surface texture induced by sequential machining processes should be developed (Grzesik et al., 2007; Grzesik and Žak, 2012). The objective of this study is to comprehensively characterize and compare surface textures of representative hard turned, belt ground and burnished surfaces using standardized 2D and 3D roughness parameters supporting by fractal dimension and motif parameters. The quantitative comparative criterion assumes the Sz roughness parameter of about 1.35  $\mu\text{m}$  for all textures generated. It should be noticed that previous investigations of the authors concerned the comparison based on the same value of the Ra(Sa) roughness parameters (Grzesik and Žak, 2012; Grzesik et al., 2014; Grzesik et al., 2015).

## 2 Experimental Details

### 2.1 Workpiece Material and Machining Conditions

Specimens were shaped in the form of rings made of a 41Cr4 ( $57\pm 1$  HRC) steel in order to reduce their mass during roughness measurements. They were initially turned to 0.4  $\mu\text{m}$  Sa roughness and subsequently CBN turned, belt ground and burnished in order to generate surfaces with the Sz roughness of about 1.3  $\mu\text{m}$ . The machine tools were Okuma Genos L200E-M CNC precision turning center, special belt grinding device described in (Grzesik et al., 2007) and ball burnishing head mounted in a turret head of a CNC lathe described in (Grzesik and Žak, 2012).

Machining conditions for cutting and abrasive operations performed were as follows:

1. High-precision hard turning (HT) (Fig. 1a) using TNGA 160408 S01030 chamfered CBN insert, cutting speed  $v_c=150$  m/min, feed rate  $f=0.05$  mm/rev, depth of cut  $a_p=0.05$  mm. Previously, surfaces were turned using the same cutting tool with the feed rate of 0.1 mm/rev and depth of cut of 0.15 mm.

2. Two step oscillation belt grinding (BG) using abrasive belts with 30  $\mu\text{m}$  and 9  $\mu\text{m}$  grains. Rotation speed of the workpiece was 900 rev/min, belt feed was 0.06 mm/rev, oscillation frequency was 12 Hz, oscillation amplitude was  $\pm 0.5$  mm, roller pressure was 2 bars. Belt grinding (Fig. 1b) was performed during 9s with supplying oil mist produced by a MQL system.

3. Ball burnishing performed using special burnishing tool equipped with  $\text{Si}_3\text{N}_4$  ceramic ball of 12 mm diameter, as shown in Fig. 1c. The burnishing load was exerted by means of controlled spring-based pressure under static ball-workpiece. Burnishing was performed with supplying a small amount of a BP Energol CS 100 machine mineral oil with the viscosity of 100  $\text{mm}^2/\text{s}$  at 400C, produced by BP Lubricants UK Ltd. The burnishing head was mounted in the turret (Fig. 1c) and due to this fact the burnishing operations were included into CNC program along with CBN turning passes. The surface finishing by means of burnishing conditions was carried out using the burnishing speed of 25 m/min and burnishing feed ( $f_b$ ) of 0.075 mm/rev. In order to generate the required burnishing load, the tool

correction of 0.25 mm was programmed in the CNC control system. All hard turning (HT) and ball burnishing (BB) operations were performed on a CNC turning center, model Okuma Genos L200E-M.

All removal and non-removal trials were repeated, each for three-times, and the average values were determined.

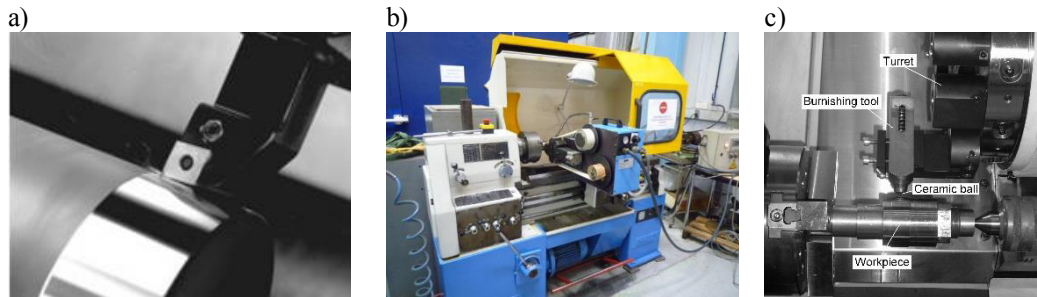


**Figure 1.** Three machining operations performed: CBN hard turning (a), belt grinding (b) and ball burnishing (c)

## 2.2 Surface Measurement Techniques

After HT, BG and BR operations the surface profiles and topographies captured on the machined surfaces were recorded using a 3D contact profilometer with a diamond stylus radius of  $2\pm 0.5\ \mu\text{m}$ . The determination of 3D roughness parameters and 3D visualization of machined surfaces were performed using a Digital Surf, Mountains® Map package. The characterization of surface topographies was based on three groups of parameters including: a) standardized 3D surface roughness parameters: height, amplitude, horizontal, hybrid and functional (Griffiths, 2001), b) fractal dimension, c) standardized motif parameters.

## 3 Experimental Results

### 3.1 Characterization of Surface Profiles and Topographies

Typical surface profiles and topographies generated in finishing hard turning (HT), abrasive (BG) and burnishing (BR) operations are presented in Figs. 1 and 2 respectively. It should be noted that in terms of the surface quality criterion all operations satisfy high-precision machining for which the maximum height  $S_z$  is about  $1\ \mu\text{m}$  (Grzesik et al., 2007).

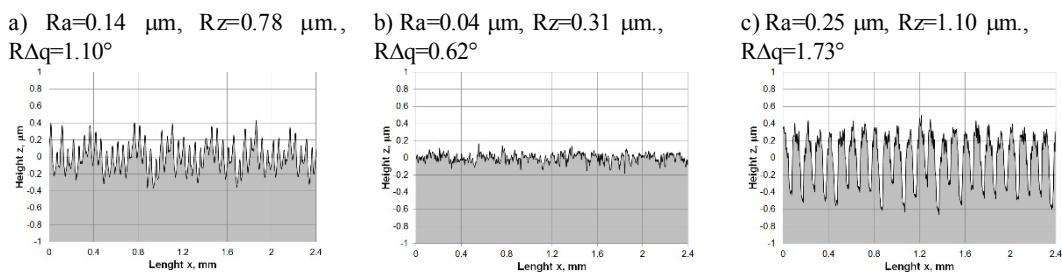


**Figure 2.** Three surface profiles generated by CBN hard turning (a), belt grinding (b) and ball burnishing (c)

Although the maximum surface height  $S_z$  is comparable (Fig. 2) the measured values of  $S_a$  oscillate between  $0.04$  and  $0.24$   $\mu\text{m}$ . As specified in Fig. 1,  $S_a$  parameter increases successively from  $0.04$   $\mu\text{m}$  for two-passes belt grinding to  $0.14$   $\mu\text{m}$  for hard turning and finally to  $0.24$   $\mu\text{m}$  for ball burnishing. On the other hand, the appropriate values of  $R_z$  parameters are not comparable due to the fact that the choice of surface profile is rather random. In this study, the 3D parameters were estimated based on about 200 profiles within the scanned area of  $2.5$   $\text{mm} \times 2.5$   $\text{mm}$ . It was the reason why the comparison of the turned and ground surface textures was not based on the constant  $R_z$  parameter as in Ref. (Davim, 2011) but on the constant  $S_z$  parameter.

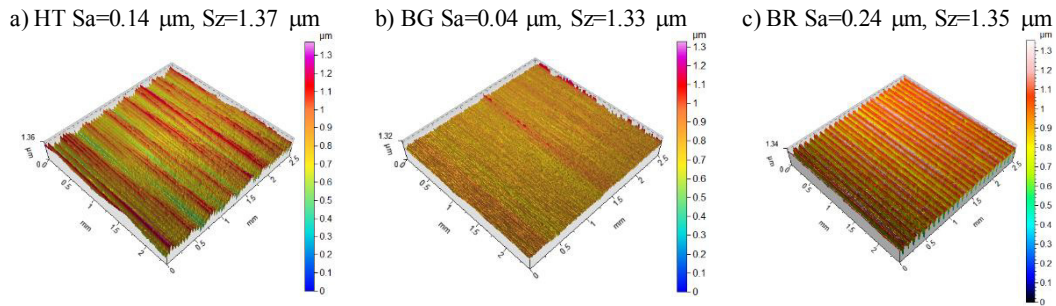


**Figure 3.** Three surface topographies generated by CBN hard turning (a), belt grinding (b) and ball burnishing (c)

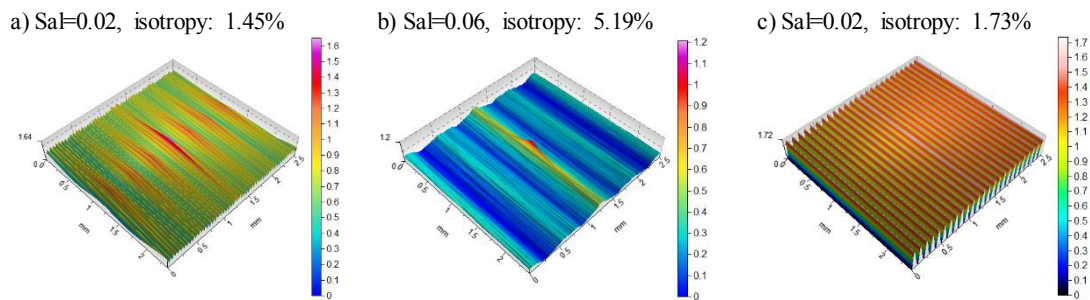


**Figure 4.** Distributions of the autocorrelation function for surfaces generated by CBN hard turning (a), belt grinding (b) and ball burnishing (c)

The strong anisotropy of all machined surfaces shown in Fig. 2 is confirmed by characteristic shapes of the autocorrelation function (AACF) presented in Fig. 4. The turned and burnished surfaces are periodic-anisotropic (Fig. 4a and c) but the ground surface is mixed, between anisotropic and random structures (Fig. 2b). Accordingly, the values of the fastest decay autocorrelation length ( $S_{al}$ ) are equal to  $0.02$  for hard turned and burnished surfaces and  $0.06$  for belt ground surface. A larger value of  $S_{al}=0.06$  for the belt ground surface indicates that it is dominated by low spatial frequency components (Hashimoto et. al., 2008).

### 3.2 Characterization of Function Related Parameters

Figure 5 presents the shapes of 3D BAC's and associated ADF curves obtained for the compared machining operations. In particular, hard turning (1) produces surfaces with positive skew  $S_{sk}=0.13$  but both belt grinding (2) and ball burnishing (3) generate surfaces with negative skew equal to  $S_{sk}(-0.07)$  for BG and  $(-0.53)$  for BR operations. Moreover, Fig. 5b suggests that hard turning and belt

grinding produced topographies with diametrically different ADF shapes which result in various bearing and contact properties. The superior bearing properties (denoted by  $S_{sk}=-0.53$ ) were obtained when sharp irregularities produced by hard turning were removed by burnishing action of the ceramic ball (BAC #3 in Fig. 5a). Additionally, values of the areal material ratio  $S_{mr}(c)$ , the inverse areal material ratio  $S_{dc}(mr)$  and the peak extreme height  $S_{xp}$  are given in Fig. 5a.

Additionally, the effect of the vectorisation of micro-valleys network generated on the machined surface is shown in Fig. 6. This technique allows assessing the fluid retention capability of the surface. The maximum depth of valleys ranges between 0.35 and 1.05  $\mu\text{m}$  and their widths are equal to 0.35  $\mu\text{m}$  for turned and burnished textures and 0.08  $\mu\text{m}$  after belt grinding and initially turned surface. Additionally, the average density of valleys is between 400 and 800  $\text{cm}^2/\text{cm}^2$  respectively. This comparison indicates that abrasive operations produce surfaces with a larger number of deeper valleys (Fig. 6b) which increases retention capability. These data coincides well with the distributions of the volume functional parameter ( $V_{mp}$  and  $V_{vv}$ ) shown in Fig. 7. The functional analysis of the 3D BAC's is based on the four volume parameters including the peak material volume ( $V_{mp}$ ), the core material volume ( $V_{mc}$ ), the core void volume ( $V_{vc}$ ) and the valley void volume ( $V_{vv}$ ) parameters (Jiang and Whitehouse, 2012; De Chiffre et al., 2000).

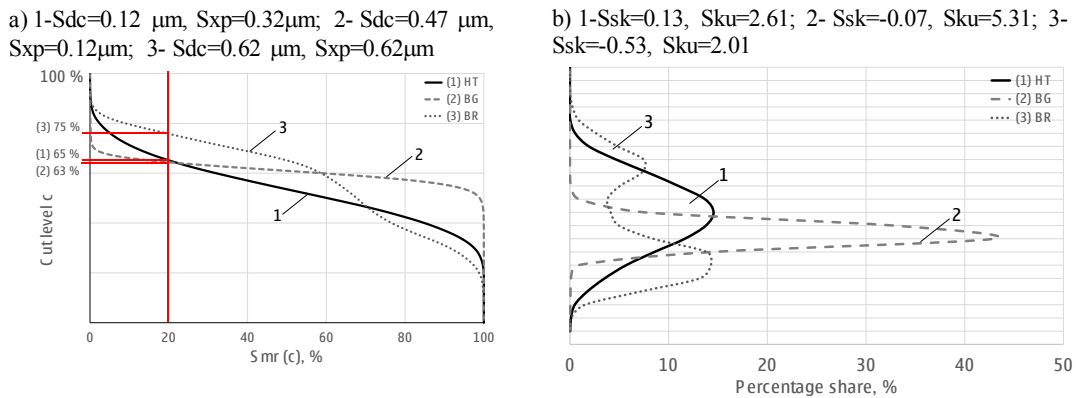


**Figure 5.** 3D BAC shapes (a) and ADF distributions (b) for turned (1), belt ground (2) and burnished (3) surfaces

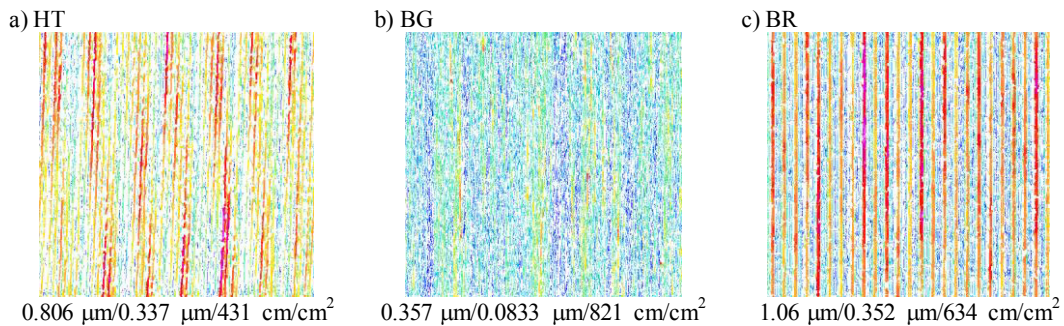


**Figure 6.** Vectorized micro-valley networks for turned (a), belt ground (b) and burnished (c) surfaces. Three values give the average depth, width and density of micro-valleys

Their values obtained for HT and abrasive operations are as follows (in order HT/BG/BR):  $V_{mp}=0.0798/0.0259/0.0433 \mu\text{m}^3/\mu\text{m}^2$ ;  $V_{mc}=0.167/0.0497/0.331 \mu\text{m}^3/\mu\text{m}^2$ ;  $V_{vc}=0.230/0.0658/0.285$

$\mu\text{m}^3/\mu\text{m}^2$ ;  $V_{vv}=0.0175/0.00723/0.0223 \mu\text{m}^3/\mu\text{m}^2$ . In particular, higher values of  $V_{vv}=0.0223 \mu\text{m}^3/\mu\text{m}^2$  confirm better fluid retention ability of burnished surfaces in comparison to turned and especially to belt ground surfaces.

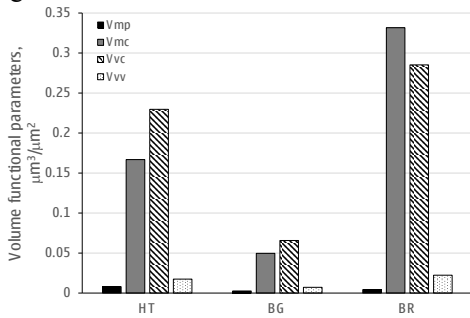


**Figure 7.** Functional volumetric parameters for different finishing operations

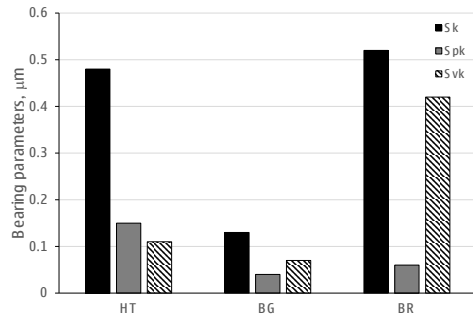


**Figure 8.** Areal bearing area parameters for different finishing operations

The function related parameters including three areal (V) material ratio parameters- the reduced core (Sk), peak (Spk) and valley (Svk) height and their ratios - Spk/Sk, Svk/Sk, Spk/Svk are compared in Figs. 8 and 9. In particular, the ratio of Spk/Sk may be helpful to distinguish between two surfaces with indistinguishable roughness average Sa (Leach, 2013). It can be seen in Fig. 8 that cutting and burnishing operations generated surfaces with comparable values of the reduced core height of about 0.5  $\mu\text{m}$  which is reduced by abrasive operation to 0.13  $\mu\text{m}$ . On the other hand, visible differences between the reduced peak (Spk) height and reduced valley (Svk) height can be observed in Fig. 8. The lowest Spk of 0.04  $\mu\text{m}$  corresponds to belt ground surfaces and the highest Svk of 0.42  $\mu\text{m}$  to burnished surfaces. In other words, belt ground surfaces have the highest wear resistance and the burnished surfaces have the best fluid retention capability.

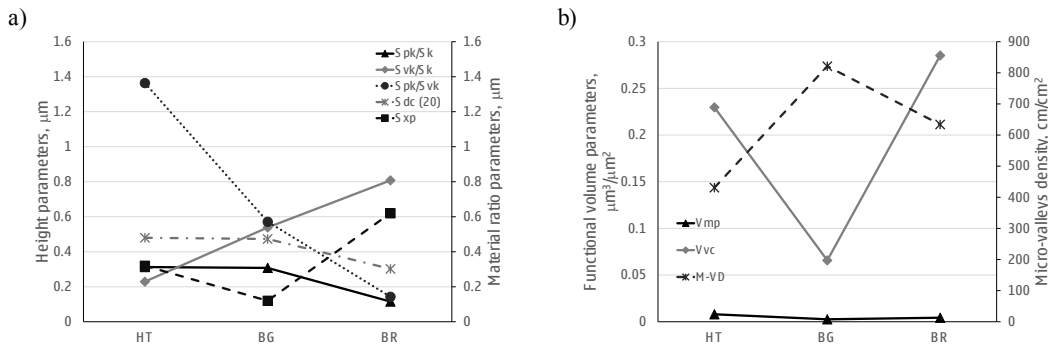


**Figure 9.** Functional relationships between selected 3D V-parameters.

Moreover, both turned and ground surfaces with the same Sz have comparable Spk/Sk values of about 0.3 (Fig. 9a). It is further reduced down to 0.115 by ball burnishing. In particular, the highest Svk/Sk ratio of about 0.8 is denoted for ball burnished surfaces with exceptional fluid retention abilities (in contrast for turned surface this ratio is about 0.2). As shown in Fig. 9b, the ratio of Spk/Sk correlates well also with the Vmp volume parameter, whereas the ratio of Svk/Sk with the Vvc volume parameter and in a lower scale with micro-valleys density. Additional relationships can be observed (Fig. 7a) between the ratio of Spk/Svk and Sdc and Sxp material ratio parameters.

### 3.3 Characterization of Spatial and Hybrid Parameters

The set of 3D parameters includes four spatial parameters, three of which are texture parameters. The ground surfaces contain distinctly more summits within the scanned area -  $S_{ds}=3001.6 \text{ 1/mm}^2$  (BG) versus  $1459.4 \text{ 1/mm}^2$  (HT) and  $1149.1$  (BR). The comparable small texture aspect ratio  $Str=0.01-0.05$  for all machined surfaces indicates stronger directionality (anisotropy) but its values for both cutting and abrasive operations, which are less than 0.1, are characteristic for highly anisotropic surfaces (Griffiths, 2001). The texture direction  $Std$  close to  $90^\circ$  for all three surfaces indicates that the dominant surface lay is perpendicular to the measurement direction. The values of  $Sal$  parameter are given in Fig. 4.

Values of three 3D hybrid parameters emphasize additional geometrical differences in the compared textures. Very low slopes  $S_{dq}$  of about 1-30 characterize very smooth surfaces (Hashimoto et al., 2008). The values of the average summit curvature  $S_{sc}$  of about  $0.005 \mu\text{m}^{-1}$  for the turned and ground surface and about  $0.008 \mu\text{m}^{-1}$  for the burnished surfaces are typical for machined surfaces ( $0.004-0.03 \mu\text{m}^{-1}$  given in (Griffiths, 2001)). The  $S_{dr}$  parameter (the developed interfacial area ratio) of 0.04% is higher for burnished surfaces (Fig. 1b and c) than for turned and ground surfaces (Figs. 1a and d)-0.02%/0.01%.

### 3.4 Motifs and Fractals

The motif analysis is performed on the unfiltered surface profile divided into a series of windows (Griffiths, 2001; Michigan Metrology) and is based on the estimation of the mean depth of roughness motif  $R$ , the mean spacing of roughness motif  $AR$  and the largest motif height  $R_x$ .

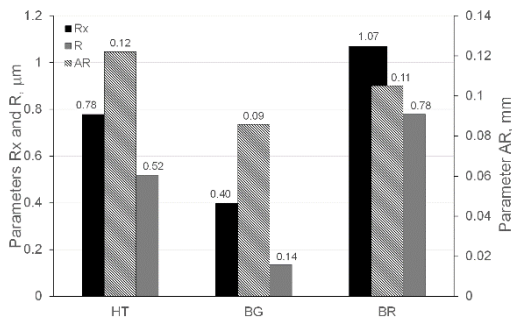


**Figure 10.** Examples of the motif graphs for hard turned (a), belt ground (b) and burnished (c) surfaces

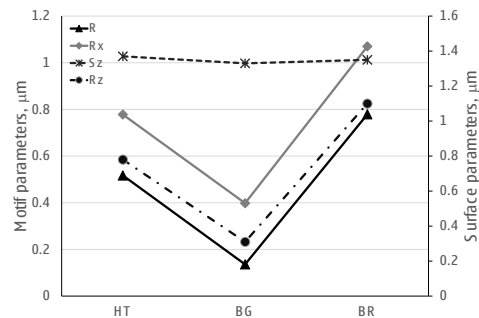


**Figure 11.** Functional relationships between  $S_z$  ( $R_z$ ) and  $R_x$ ( $R$ ) motif parameters

As shown in Fig. 10 burnished surfaces include distinctly deeper pits ( $R_x=1.07 \mu\text{m}$ ) than hard-turned and belt ground surfaces ( $R_x=0.70/0.40 \mu\text{m}$ ) which is in accordance with volume bearing parameters (Fig. 8). Fig. 11 shows that the  $R_x$  motif parameter is stronger correlated with the  $R_z$  parameter rather than  $S_z$  because motifs are based on 2D analysis. Moreover, the  $R$  motif parameter of  $0.14-0.78 \mu\text{m}$  is also independent of the machining operations used and coincides with the  $R_z$  changes.

The values of fractal dimension  $S_{fd}$  determined by means of the method of enclosing boxes are equal to 2.40, 2.54 and 2.38 for turned, ground and burnished surfaces subsequently. Functional relationships between fractal dimension  $S_{fd}$  and  $Sal$ ,  $S_{sc}$  and  $S_{ds}$  spatial and hybrid parameters were revealed in Fig. 12. It can be noticed in Fig. 12a that the  $S_{fd}$  is strongly correlated with the density of summits ( $S_{ds}$ ) and  $S_{fd}=2.54$  corresponds with the maximum value of  $S_{ds}=3001.6 \text{ 1/mm}^2$  determined for the belt ground surface. At the second order, it deals with the arithmetic summit curvature ( $S_{sc}$ )

and the autocorrelation length  $S_{al}$  parameter which characterize the uniformity of the texture (Fig. 12b).

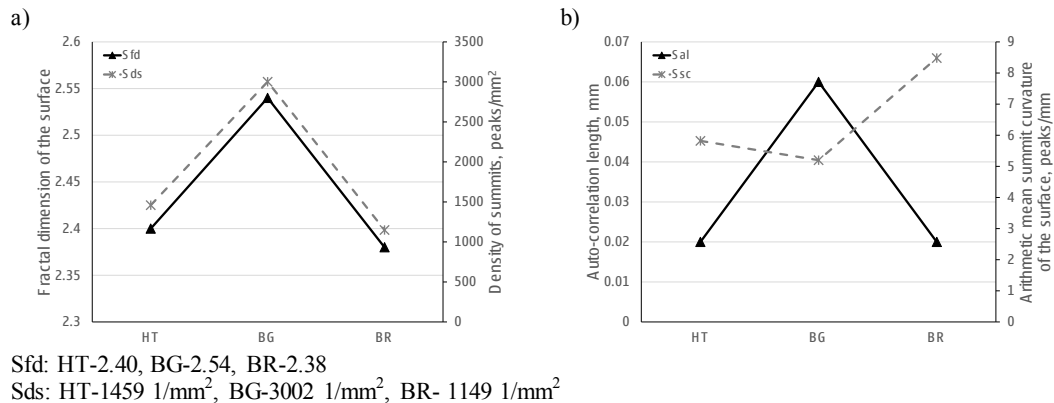


**Figure 12.** Functional relationships between selected 3D S-parameters and fractal dimension

## 4 Conclusions

This study clearly indicates how high-precision machining operations can be performed in order to obtain desired surface texture and functional properties, i.e. resistant to wear, fluid retention ability, resistant to contact loads, etc.

The following specific comments are formulated based on the measured data and analyses carried out.

1. Although attributes of turned, ground and burnished surfaces are described by the same height  $S_z$  parameter of about 1.3  $\mu\text{m}$  their spatial features and functional properties are, in some cases, distinctly different.

2. The distributions of the PSD (APSD) function and vectorial maps of micro-valleys suggest that the textures of hard turned and burnished surfaces are periodic-anisotropic. On the other hand, the structures of ground surfaces are random anisotropic.

3. 3D BAC curves and appropriate functional parameters indicate that smooth burnished hard surfaces have enhanced fluid retention abilities. This is due to a large negative  $S_{sk}$  value and higher  $V_{vv}$  volumes for burnished textures.

4. Hard belt ground and burnished textures have comparable  $V_{mp}$  and  $S_{pk}$  parameters and as a result comparable tribological properties. The best tribological performance of the belt ground surface is due to minimum  $V_{mp}$  and  $S_{pk}$  values.

## References

- Davim JP. *Machining of hard materials*. London: Springer, 2011.
- De Chiffre L, Lonardo PM, Trumpold H, Lucca DA, Goch G, Brown CA, Raja J and Hansen HN. Quantitative characterization of surface texture. *CIRP Annals-Manufacturing Technology* 2000; 49 (2): 635-652.
- Griffiths, B. *Manufacturing surface technology. Surface integrity and functional performance*. London: Penton Press, 2001.



Grzesik W, Rech J, and Wanat T. Surface finish on hardened bearing steel parts produced by superhard and abrasive tools. *International Journal of Machine Tools and Manufacture* 2007; 47(2): 255-262.

Grzesik W and Żak K. Modification of surface finish produced by hard turning using superfinishing and burnishing operations. *Journal of Materials Processing Technology* 2012; 212(1): 315-322.

Grzesik W, Żak K and Kiszka P. Comparison of surface textures generated in hard turning and grinding operations. *Procedia CIRP* 2014; 13: 84-89.

Grzesik W and Żak K. Possibilities of the generation of hardened steel parts with defined topographic characteristics of the machined surfaces. *Journal of Manufacturing Science and Engineering* 2015; 137(1): 014502-1-014502-5. doi: 10.1115/1.4028895

Hashimoto F, Guo YB and Warren AW. Surface integrity difference between hard turned and ground surfaces and its impact on fatigue life. *Annals of the CIRP* 2008; 55(1): 81-84.

Jiang XJ and Whitehouse DJ. Technological shifts in surface metrology. *CIRP Annals-Manufacturing Technology* 2012; 61(2): 815-836.

Klocke F, Brinksmeier E and Weinert K. Capability profile of hard cutting and grinding processes. *CIRP Annals-Manufacturing Technology* 2005; 54(2): 557-580.

Klocke F. *Manufacturing processes I. Cutting*. Berlin: Springer, 2011.

König W, Berktold A and Koch KF. Turning versus grinding- a comparison of surface integrity aspects and attainable accuracies. *CIRP Annals-Manufacturing Technology* 1993; 42(1): 39-43.

Leach R. *Characterization of areal surface texture*. Berlin: Springer-Verlag, 2013.

Lonardo PM, Trumpold H and De Chiffre L. Progress in 3D surface microtopography characterization. *CIRP Annals-Manufacturing Technology* 1996; 45(2): 589-598.

Michigan Metrology, *3D surface roughness and wear measurements, analysis and inspection*. Available at [www.michmet.com](http://www.michmet.com).

Tönshoff HK, Arendt C and Ben Amor C. Cutting of hardened steel. *CIRP Annals-Manufacturing Technology* 2000; 49(2): 547-566.